

# Expected statistical uncertainties of $\pi$ -induced Drell-Yan cross sections with Tungsten target at COMPASS

C.-Y. HSIEH<sup>1,2</sup> on behalf of the COMPASS Collaboration,

<sup>1</sup>*Institute of Physics, Academia Sinica, Taipei, Taiwan*

<sup>2</sup>*Department of Physics, National Central University, Taoyuan, Taiwan*

*E-mail: cyhsieh@phys.sinica.edu.tw*

(Received Jan. 18, 2019)

The Drell-Yan production from 190-GeV  $\pi^-$  beams interacting with a tungsten target was measured by the CERN COMPASS experiment. We present the expected statistical errors of the differential cross sections as a function of  $x_F$  in two  $\sqrt{\tau}$  regions and the comparison with the results of E615 experiment.

**KEYWORDS:** Drell-Yan process, pion, parton density functions

## 1. Drell-Yan Measurement at COMPASS

The COMPASS collaboration performs fixed-target experiments at the north area of CERN SPS in Geneva, Switzerland. COMPASS studies the hadron structure and hadron spectroscopy using high-intensity muon and hadron beams together with various unpolarized/polarized targets. From a measurement with a transversely polarized target, COMPASS extracted information on Sivers functions for the first time via the Drell-Yan process [1]. In this work, the aim is for the measurement of Drell-Yan differential cross section from the unpolarized targets [2] and this information is crucial for the global analysis of pion parton density functions (PDFs) [3].

The setup for Drell-Yan runs in 2015 and 2018 is shown in Fig. 1. The hadron beam delivered by the SPS to COMPASS has an intensity of  $6 \times 10^7$  particle/s. The beam is composed of 97%  $\pi^-$ , 2.5%  $K^-$ , and 1%  $p^-$ . Three kinds of targets, Al,  $\text{NH}_3$  and W, were used. In order to detect the dimuon pairs from high-energy Drell-Yan processes, a hadron absorber is installed to stop the produced hadrons from entering the spectrometer. COMPASS uses a two stage spectrometer. The large angle spectrometer (LAS) detects the charged tracks with a scattering angle between 35 mrad and 180 mrad. The second stage is the small angle spectrometer (SAS) covering tracks with scattering angle between 18 mrad and 35 mrad.

## 2. Analysis

The Feynman diagram of Drell-Yan process at Leading Order (LO) is sketched in Fig. 2. The kinematic variables of Drell-Yan process are defined as in Table. I. The differential cross section per nucleon as a function of the kinematic variables  $x$  and  $y$  is expressed as

$$\frac{d^2\sigma}{dx dy} = \frac{dN_{\mu^+\mu^-}}{dx dy} \times \frac{1}{\mathcal{E}_{\text{MC}} \mathcal{E}_{\text{trig}} \mathcal{E}_{\text{veto}} \mathcal{E}_{\text{DAQ}}} \times \frac{1}{\mathcal{L}} \times \frac{1}{A} \quad (1)$$

, where  $N_{\mu^+\mu^-}$  is the number of selected Drell-Yan events. The  $\mathcal{E}_{\text{MC}}$  is the efficiency evaluated by Monte-Carlo (MC) including geometrical acceptance, detector efficiency, track reconstruction efficiency, event selection efficiency. In addition, there are trigger efficiency  $\mathcal{E}_{\text{trig}}$ , beam veto life time

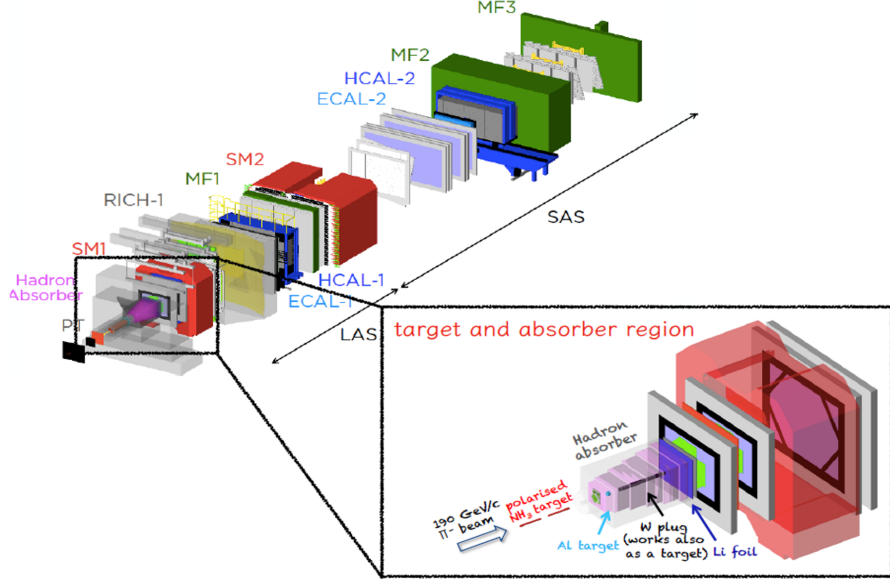


**Fig. 1.:** Setup for Drell-Yan runs at COMPASS.

$\mathcal{E}_{\text{veto}}$  and DAQ life time  $\mathcal{E}_{\text{DAQ}}$  to account for the dead time introduced by vetoing halo beam particles entering the experimental area and the dead time introduced by the acquisition system.  $\mathcal{L}$  is the integrated luminosity (in the unit of  $\text{cm}^{-2}$ ).  $A$  is a number of nucleons per unit area in the target system.

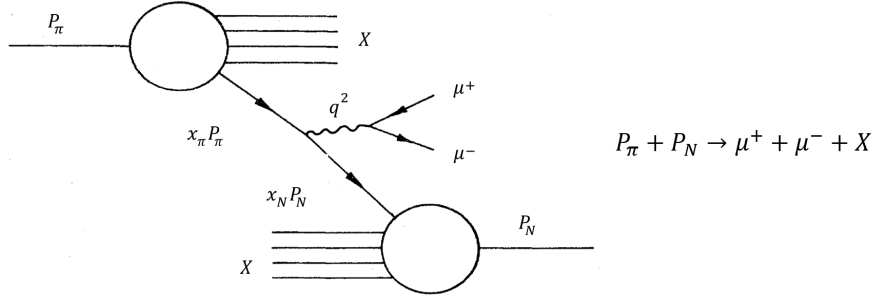


**Fig. 2.:** Feynman diagram of Drell-Yan process at leading order (LO).

Drell-Yan events with a dimuon invariant mass  $M_{\mu^+\mu^-}$  between 4.3 and 8.5  $\text{GeV}/c^2$  are selected. The vertex distribution along the longitudinal coordinate  $z$  for the selected events is shown in Fig. 3. The five peaks correspond to the Drell-Yan reactions taking place in the two  $\text{NH}_3$  cells, the vertex detector, the Al target and the  $W$  beam plug, respectively. The highlighted blue areas in the figure correspond to the target selection. For example, only the first 10 cm of  $W$  target was considered to avoid the contribution from secondary re-interaction.

### 3. Expected statistical uncertainties

The event yields as a function of  $\sqrt{\tau}$  (fraction of energy between hadron system and muon system) from the first 10-cm of  $W$  target are shown in Fig. 4. In order to compare with the results of E615 experiment [2], two regions of  $0.277 < \sqrt{\tau} < 0.323$  and  $0.323 < \sqrt{\tau} < 0.369$  are selected for

**Table I.** Table of kinematic variables

Variable	Description
$P_\pi, P_N$	4-momenta of the beam pion, and of the target nucleon
$P_{\mu^+}, P_{\mu^-}$	4-momenta of the single muon
$P = P_\pi + P_N$	4-momenta of the hadron system
$q = P_{\mu^+} + P_{\mu^-}$	4-momenta of the virtual photon
$M_{\mu^+\mu^-} = \sqrt{q^2}$	invariant mass of the dimuon pair
$\sqrt{s} = \sqrt{P^2}$	center of mass energy of hadron system
$q_T$	transverse component of the virtual photon momentum
$x_\pi = q^2/(2P_\pi \cdot q)$	Bjorken- $x$ of partons from pion beam
$x_N = q^2/(2P_N \cdot q)$	Bjorken- $x$ of partons from target nucleon
$x_F = x_\pi - x_N$	Feynman- $x$
$\sqrt{\tau} = \sqrt{q^2/P^2} = \sqrt{x_\pi x_N}$	fraction of energy between hadron system and muon system

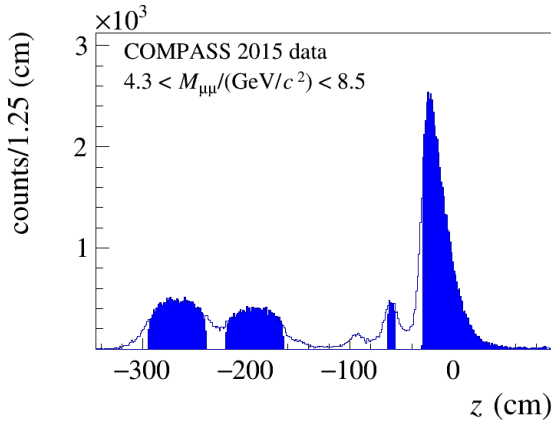


**Fig. 3.:** Vertex- $z$  distribution of the Drell-Yan events.

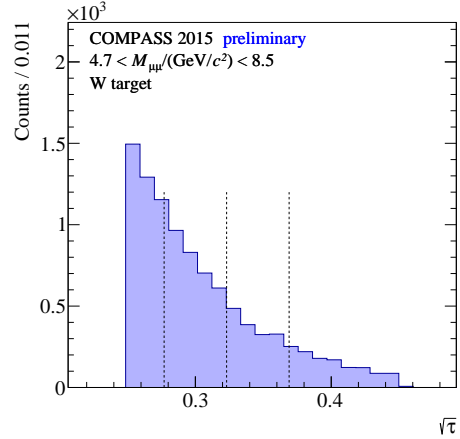


**Fig. 4.:** The  $\sqrt{\tau}$  distributions of selected dimuons events from the first 10 cm region of W target.

study. The expected statistical uncertainties and the relative uncertainties of differential cross section as a function of  $x_F$  for W target are shown in Fig. 5 and Fig. 6, respectively.

In Fig. 5, all the distributions including DYNNLO calculation (green band), E615 cross section (blue-open circles), and expected statistical uncertainty of COMPASS (red-full squares) are scaled by the square of the center-of-mass energy in order to have energy-independent comparison. The expected statistical uncertainties of COMPASS for the two intervals of  $\sqrt{\tau}$  are evaluated with the event yields normalized by the expected cross sections from the fixed-order Drell-Yan calculations with DYNNLO and MCFM Monte-Carlo packages [4–6]. The GRV-NLO [3] and CT14-NLO [7] are used for the pion and proton PDFs, taking into account the isospin components of W nuclei. The uncertainty band is using the PDFs uncertainties. The E615 data are consistent with the results of the fixed-order Drell-Yan calculations. In Fig. 6, the relative uncertainties are also shown.

We conclude that the statistical accuracy of 2015 DY data is slightly better than that of E615 data, except for the large  $x_F$  region. COMPASS had another Drell-Yan run in 2018 and a factor of 1.5 more statistics were collected which will increase accordingly the precision for the 2015-2018 combined results.

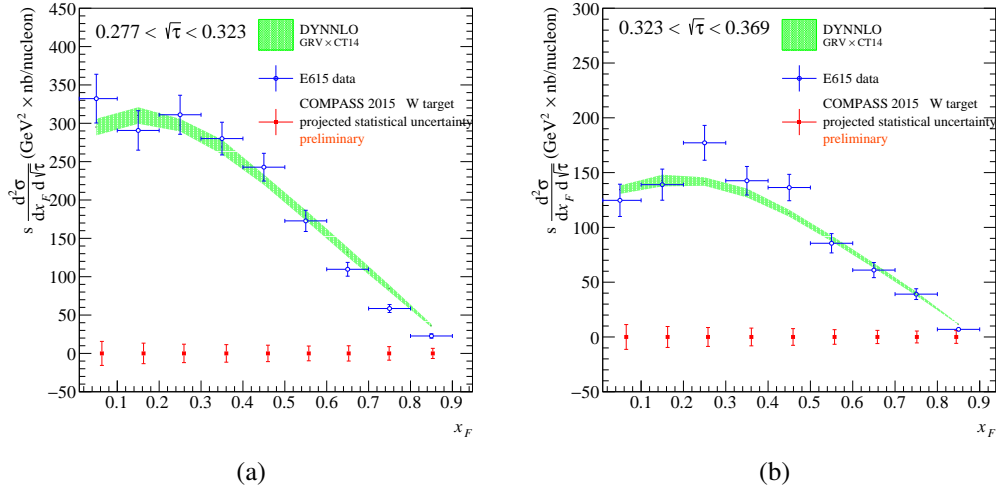


**Fig. 5.:** The expected statistical uncertainties of Drell-Yan differential cross sections of  $W$  target in  $x_F$ . (a)  $0.277 < \sqrt{\tau} < 0.323$ . (b)  $0.323 < \sqrt{\tau} < 0.369$ .

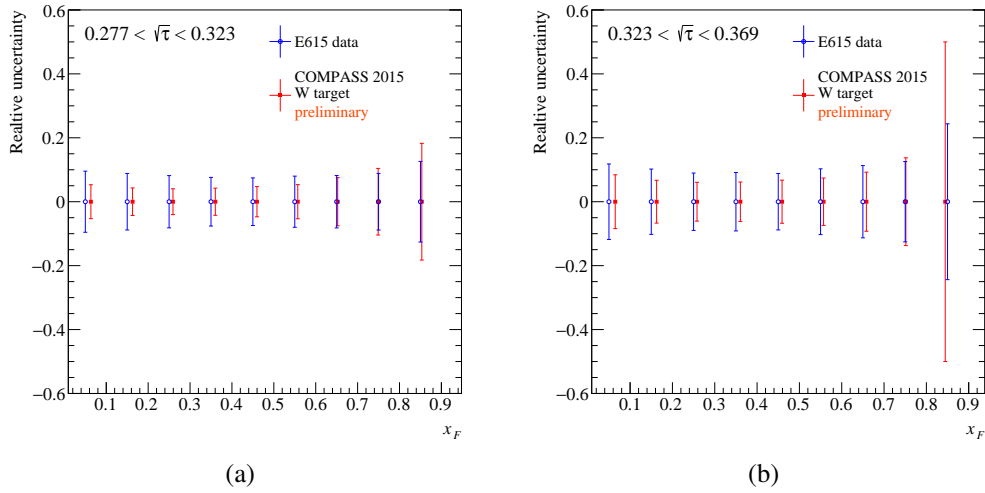


**Fig. 6.:** The relative uncertainties of Drell-Yan differential cross sections of  $W$  target in  $x_F$ . (a)  $0.277 < \sqrt{\tau} < 0.323$ . (b)  $0.323 < \sqrt{\tau} < 0.369$ .

## References

- [1] COMPASS Collaboration, M. Aghasyan *et al.*, Phys. Rev. Lett. **119**, 112002 (2017).
- [2] E615 Collaboration, J. S. Conway, *et al.*, Phys. Rev. D**39** (1989) 92.
- [3] M. Glück, E. Reya and A. Vogt, Z. Phys. A, C**53** (1992) 651.
- [4] S. Catani, *et al.*, Phys. Rev. Lett. **103** (2009) 082001.
- [5] S. Catani and M. Grazzini, Phys. Rev. Lett. **98** (2007) 222002.
- [6] R. Boughezal, *et al.*, Eur. Phys. J. C**77** (2016) 1.
- [7] T. J. Hou *et al.*, JHEP **099** (2017) 099.
- [8] K. J. Eskola, *et al.*, Eur. Phys. J. C**9** (1999) 61.